

# Performance of gain-switched Ti:Al<sub>2</sub>O<sub>3</sub> unstable-resonator lasers

Glen A. Rines and Peter F. Moulton

Schwartz Electro-Optics, Inc., 45 Winthrop Street, Concord, Massachusetts 01742

Received September 29, 1989; accepted February 12, 1990

We describe an experimental investigation of Ti:Al<sub>2</sub>O<sub>3</sub> unstable-resonator lasers. A near-diffraction-limited output of 430 mJ in a 10-nsec pulse at 10 Hz has been obtained, which is to our knowledge the highest peak power from a Ti:Al<sub>2</sub>O<sub>3</sub> laser reported. We report results for both standing-wave and traveling-wave oscillators, demonstrating line narrowing by means of prism tuning and injection seeding.

Ti:Al<sub>2</sub>O<sub>3</sub> is a broadly tunable, solid-state laser medium that has been studied extensively since laser operation was first demonstrated in 1982.<sup>1</sup> In this Letter we report the generation of high-peak-power outputs from Ti:Al<sub>2</sub>O<sub>3</sub> lasers configured with unstable-resonator cavities.<sup>2</sup> Spectral line narrowing of the output has been obtained by injection seeding from a cw Ti:Al<sub>2</sub>O<sub>3</sub> laser. Our experiments were performed with a Q-switched, frequency-doubled, Nd:YLF pump laser, which led to a gain-switched, single-pulse output from the Ti:Al<sub>2</sub>O<sub>3</sub> system. Historically, experiments with gain-switched Ti:Al<sub>2</sub>O<sub>3</sub> oscillators began with stable resonators.<sup>3-5</sup> However, stable resonators cannot provide more than tens of millijoules of diffraction-limited output energy before reaching a practical limit owing to optical damage. As with other laser media, unstable resonators provide a simple, compact means of increasing the output energy of diffraction-limited oscillators.

Our 10-Hz, Nd:YLF pump laser provided a nominal 20-nsec, multitransverse-mode, linearly polarized beam. Using this pump, we carried out a series of experiments with positive-branch, confocal unstable resonators in standing-wave and ring configurations. Three types of output coupler for the unstable resonators were investigated: high-reflectivity dot mirrors (HRDM's), partial-reflectivity dot mirrors (PRDM's), and graded-reflectivity mirrors (GRM's).

Schematics for the standing-wave and ring resonators used are shown in Fig. 1. The two-mirror, positive-branch configuration in Fig. 1(a) was used for the standing-wave HRDM and the GRM unstable resonator. The four-mirror resonator in Fig. 1(b) is an asymmetric, positive-branch ring design. This was the test bed for the PRDM output coupler and for the first injection-seeding experiment.

In the two-mirror HRDM experiment a very high magnification ( $M = 6.7$ ) was used to minimize diffraction effects, thereby enhancing both near- and far-field profiles. (The high single-pass gains that can be attained in Ti:Al<sub>2</sub>O<sub>3</sub> permit the use of such a high output coupling.) The PRDM output coupler, a 60%  $R$ , 2-mm-diameter dot, was used in a low-magnification ring resonator ( $M = 1.67$ ). This design was chosen to make the coating deposition more practical (2 mm versus 0.75 mm for the HRDM experiment) while

reasonable feedback was maintained. The diffraction problem associated with low magnification is mitigated to some degree by the PRDM design combined with the soft gain aperture inherent in the laser-pumped Ti:Al<sub>2</sub>O<sub>3</sub> oscillator. The more recent experiments were performed with a GRM design, which minimizes diffraction effects and produces a smooth spatial profile in both the near and far fields. The reflectivity profile of the GRM used in this experiment was parabolic with an exponential tail similar to that used in recent Nd:YAG experiments.<sup>6</sup> The reflectivity profile is given by

$$R = R_0[1 - (r/0.91 \text{ mm})^3] \quad \text{for } r \leq 0.86 \text{ mm},$$

$$R = \exp[-13(r - 0.62 \text{ mm})] \quad \text{for } r > 0.86 \text{ mm},$$

where  $r$  is the radial distance from the mirror center and  $R_0$  is the center reflectivity coefficient (0.27).

The performance of these three unstable resonators is summarized in Table 1. Since both the pulse width and the pulse buildup time are important to the understanding of gain-switched oscillators, we have measured these parameters for use in future modeling and

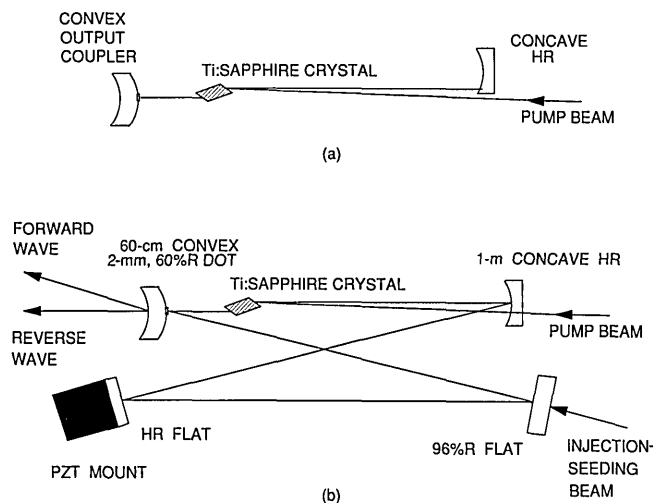


Fig. 1. Schematics of the resonators used in the Ti:Al<sub>2</sub>O<sub>3</sub> oscillator experiments: (a) standing-wave, positive-branch resonator; (b) asymmetric, positive-branch, unstable ring resonator. HR, high-reflectivity mirror; PZT, piezoelectric translator.

**Table 1. Summary of Ti:Al<sub>2</sub>O<sub>3</sub> Unstable-Resonator Data**

	Resonator Type		
	Standing Wave	Ring	Standing Wave
Magnification	6.7	1.67	1.65
Resonator length (cm)	78	195	99
Output-coupler type	HRDM	PRDM	GRM
Ti:Al <sub>2</sub> O <sub>3</sub> crystal length (cm)	1.5	1.5	1.5
Pump absorbed (%)	75	96	96
Ti:Al <sub>2</sub> O <sub>3</sub> figure of merit	28	>100	>100
Maximum output (mJ)	90	180	430
Maximum pump (mJ)	350	500	1000
Ratio over threshold	2.7	2.6	5.3
Output limited by	Available pump	Available pump	Ti:Al <sub>2</sub> O <sub>3</sub> damage
Conversion efficiency (%)	26	36	43
Pulse width at maximum output (nsec)	7	24	≈10
Pulse buildup at maximum output (nsec)	28	85	≈20

analysis. The pulse buildup data and pulse width as a function of the ratio over threshold are shown in Figs. 2 and 3, respectively.

During the HRDM and PRDM experiments, our analysis of spatial profiles of the output beams was limited to the qualitative observation of burn patterns on film emulsions. During some of the GRM experiments near- and far-field spatial profiles were monitored with a silicon charge-coupled-device camera and recorded on a computer for analysis. The far-field profiles were taken by placing a camera monitor at the focal plane of a 1-m lens. The beam divergence values measured typically are between 1.5 and 2.5 times the diffraction limit, as defined by Gaussian fits to the near- and far-field beam profiles. Samples of the near- and far-field spatial profiles of a GRM resonator are shown in Fig. 4, along with a Gaussian fit to the near-field data.

The smooth profile of the GRM oscillator to both the near and far fields is a distinct advantage over the profiles of the other output couplers. The HRDM oscillator produced a doughnut profile in the near field with an 0.75-mm hole in the center. In the near field the typical PRDM oscillator burn pattern was a 3.5-mm-diameter circle with a 2-mm central disk, an annular dark ring of ≈0.3 mm diameter, and an 0.9-mm outer ring.

The two-mirror resonator used for the GRM experiments was modified to explore the utility of intracavity prisms for tuning and line narrowing. Three equilateral BK-7 prisms were placed in the cavity near the Brewster-cut Ti:Al<sub>2</sub>O<sub>3</sub> crystal and set at the minimum deviation angle for 800 nm. The unstable resonators containing only the Brewster-cut Ti:Al<sub>2</sub>O<sub>3</sub> as a dispersive element had spectral linewidths varying from 20 to 30 nm (FWHM). The three-prism cavity linewidth was reduced to 0.7 nm. In addition, smooth wavelength tuning over the mirror bandwidth was ob-

tained by adjusting the azimuthal angle of the resonator mirrors.

The ultimate line narrowing for these resonators can be produced by injection seeding with a single-frequency, cw Ti:Al<sub>2</sub>O<sub>3</sub> laser. Two injection-seeding experiments have been done to date with a cw Ti:Al<sub>2</sub>O<sub>3</sub> ring resonator, the design of which has been reported elsewhere.<sup>2</sup> The cw seeding laser had a spectral linewidth of <1 MHz. The unstable ring configuration shown in Fig. 1(b) was used for the first seeding experiment. Ultimately the seed beam may be injected through the output coupler. However, in this experiment the seed was injected through a 96% R cavity mirror.

During the first seeding experiment, we monitored the Ti:Al<sub>2</sub>O<sub>3</sub> laser output with a 1024-element detector array at the image plane of a spectrometer. With this low-resolution monitor the dramatic collapse of the nominal 20-mm (FWHM) free-running linewidth was readily observed. Figure 5 shows the free-running spectrum along with the narrow injection-seeded spectrum. In addition to the line narrowing, the seed beam effectively forced unidirectional operation of the ring. In the unseeded case the output energy for the

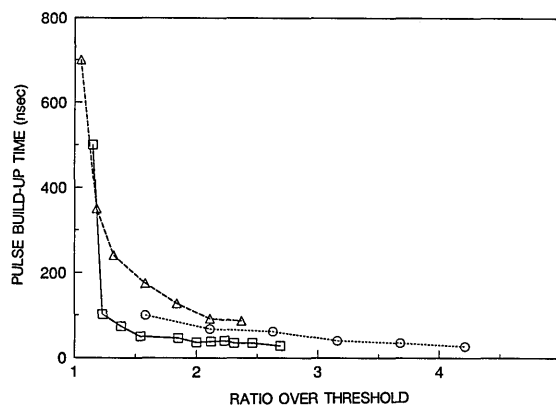


Fig. 2. Pulse buildup time data for the three resonators described in Table 1. Squares, standing-wave HRDM ( $M = 6.7$ ); triangles, ring PRDM ( $M = 1.67$ ); circles, standing-wave GRM ( $M = 1.65$ ).

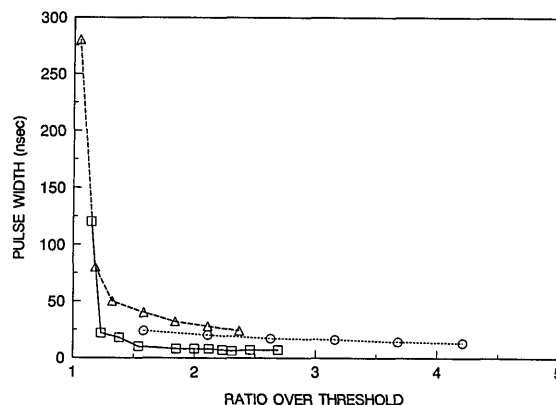


Fig. 3. Pulse-width data for the three resonators described in Table 1. Squares, standing-wave HRDM ( $M = 6.7$ ); triangles, ring PRDM ( $M = 1.67$ ); circles, standing-wave GRM ( $M = 1.65$ ).

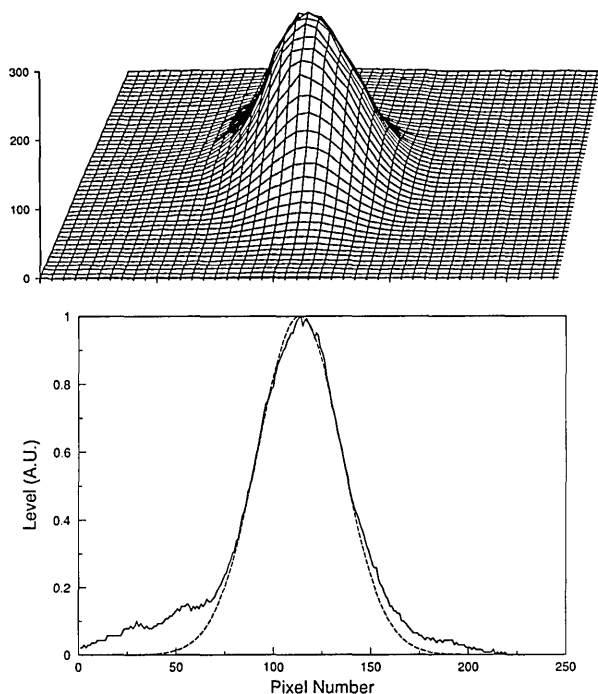


Fig. 4. (Top) Far-field two-dimensional intensity spatial profile of the GRM unstable-resonator output and (bottom) a near-field one-dimensional intensity profile (the solid curve) taken through the center of the beam and a Gaussian fit (the dashed curve).

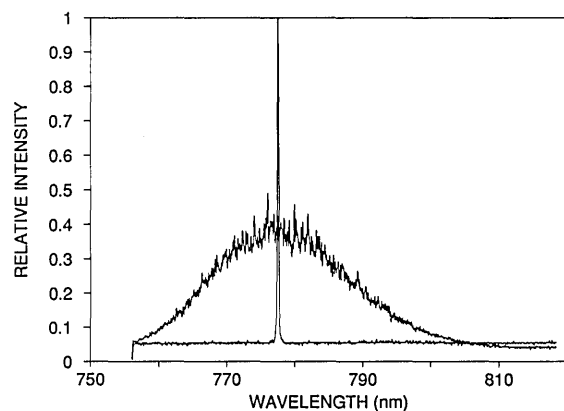


Fig. 5. Wavelength spectra of the unstable ring resonator shown in Fig. 1(b) with and without injection seeding.

ring was evenly split between the forward and reverse waves, while in the presence of the seed beam the forward-wave output increased to twice the unseeded value, the reverse wave dropped to zero, and the line-narrowed spectrum appeared.

We did the first seeding experiment with a 150-mW seed beam and without spatial mode matching to the slave resonator. Under these conditions seeding occurred only with appropriate tuning of either the resonator length or the seed wavelength, demonstrating that there was a finite seeding bandwidth that was less

than the axial-mode spacing (154 MHz) in the slave resonator.

We also performed a seeding experiment with a standing-wave GRM resonator in which we were able to obtain seeding continuously with  $\approx 500$  mW of seed power incident upon the unstable-resonator high reflector. The resonator used for this experiment was similar to the one described in Table 1 but with a cavity length of 150 cm (axial-mode spacing of 100 MHz). As in the PRDM ring seeding experiment, the output of the cw Ti:Al<sub>2</sub>O<sub>3</sub> laser was sent directly to the slave oscillator without any attempt to mode match it to the unstable resonator. During the second experiment we monitored the temporal profile of the gain-switched Ti:Al<sub>2</sub>O<sub>3</sub> pulse and the ring pattern of a flat-flat Fabry-Perot interferometer to determine the spectral purity of the seeded pulse. Under these conditions the output exhibited the properties of a true single-frequency beam (smooth temporal profile and a clean Fabry-Perot ring pattern) on  $\sim 20\%$  of the shots. The remaining shots, while extremely narrow line, showed the strong temporal modulations produced by mode beating with secondary axial modes. With greater attention to mode matching and improvements in the seed input transmission, we expect the threshold for seeding to be reduced and the intermittent lasing of multiple axial modes to be eliminated.

In summary, we have demonstrated the utility of unstable resonators as an efficient means of generating high-energy, narrow-linewidth, fundamental-mode outputs from gain-switched Ti:Al<sub>2</sub>O<sub>3</sub> lasers. A simple prism-tuned resonator has been shown to reduce the linewidth significantly and to provide convenient wavelength tuning. The injection seeding of a ring laser has been demonstrated, showing the potential for using this technique to produce high-energy, single-frequency, near-diffraction-limited Ti:Al<sub>2</sub>O<sub>3</sub> laser output.

This research was supported by the NASA Langley Research Center, Hampton, Virginia. The Ti:Al<sub>2</sub>O<sub>3</sub> laser crystals were obtained from Union Carbide, Washougal, Washington. The Q-switched Nd:YLF pump laser was constructed in a cooperative effort with Sanders Associates, Nashua, New Hampshire.

## References

1. P. F. Moulton, Solid State Research Rep. DTIC AD-A124305/4 (MIT Lincoln Laboratory, Lexington, Mass., 1982), pp. 15-21.
2. Initial results were reported by G. A. Rines, P. F. Moulton, and J. Harrison, in *Tunable Solid-State Lasers*, Vol. 5 of OSA Proceedings Series, M. L. Shand and H. P. Jenssen, eds. (Optical Society of America, Washington, D.C., 1989), p. 2.
3. N. P. Barnes and D. K. Remelius, *Tunable Solid-State Lasers For Remote Sensing* (Stanford U. Press, Stanford, Calif., 1984), Vol. 51, pp. 78-81.
4. G. F. Albrecht, J. M. Eggelston, and J. J. Ewing, *Opt. Commun.* **52**, 401 (1985).
5. P. F. Moulton, *J. Opt. Soc. Am. B* **3**, 125 (1986).
6. A. Parent and P. Lavigne, *Opt. Lett.* **14**, 399 (1989).